Available online at www.sciencedirect.com
ScienceDirect
Journal of the European Ceramic Society 31 (2011) 2827–2837
www.elsevier.com/locate/jeurceramsoc

Field assisted and flash sintering of alumina and its relationship to conductivity and MgO-doping

Marco Cologna *, John S.C. Francis, Rishi Raj

Department of Mechanical Engineering, University of Colorado at Boulder, Boulder, CO 80309-0427, United States

Received 20 April 2011; received in revised form 14 June 2011; accepted 1 July 2011
Available online 27 July 2011

Abstract

We show that flash-sintering in MgO-doped alumina is accompanied by a sharp increase in electrical conductivity. Experiments that measure conductivity in fully dense specimens, prepared by conventional sintering, prove that this is not a cause-and-effect relationship, but instead that the concomitant increase in the sintering rate and the conductivity share a common mechanism. The underlying mechanism, however, is mystifying since electrical conductivity is controlled by the transport of the fastest moving charged species, while sintering, which requires molecular transport or chemical diffusion, is limited by the slow moving charged species. Joule heating of the specimen during flash sintering cannot account for the anomalously high sintering rates. The sintering behavior of MgO-doped alumina is compared to that of nominally pure-alumina: the differences provide insight into the underlying mechanism for flash-sintering. We show that the pre-exponential in the Arrhenius equation for conductivity is enhanced in the non-linear regime, while the activation energy remains unchanged. The nucleation of Frenkel pairs is proposed as a mechanism to explain the coupling between flash-sintering and the non-linear increase in the conductivity.

Keywords: Flash-sintering; SPS; FAST; Al_2O_3; Conductivity

1. Introduction

In recent experiments it was shown that nanocrystalline tetragonal yttria stabilized zirconia (3YSZ) can be sintered at ~850 °C in <5 s, with an electric field of 120 V cm^{-1}.[1] This phenomenon is being called flash-sintering. It is different from nominal field-assisted sintering where the application of fields leads to a gradual enhancement in the sintering rate. In 3YSZ flash-sintering occurs above a threshold field and temperature, e.g. 850 °C and 120 V cm^{-1}; while nominal field assisted sintering occurs at lower fields and higher temperatures.[1,2] Flash-sintering has been demonstrated in several oxides including, cubic yttria doped zirconia (8YSZ),[3] cobalt manganese oxide (Co_2MnO_4),[4] titanium oxide (TiO_2) and strontium titanate ($SrTiO_3$).[5,6]

The phenomenon of flash-sintering is characterized by two experimental observations: (i) at a certain temperature and applied electrical field there is a sudden increase in the sintering rate such that sintering occurs in just a few seconds. A higher applied field lowers the temperature for the onset of flash-sintering. (ii) The sintering event is accompanied by a sharp increase in the conductivity of the ceramic, which occurs at the same temperature and applied field.

An immediate interpretation of flash-sintering is that the Joule heating of the specimen precipitated by the surge in power dissipation is responsible for the very high rates of sintering. However, the measurement of the temperature during the flash event (with an optical pyrometer[7]) shows that the specimen remains far below the temperature where the ceramic would have been expected to sinter in just a few seconds. Thus, the power surge, and the surge in the sintering rate are not linked by a cause-and-effect relationship; instead they appear to share a common underlying mechanism. The exposition of this mechanism is the main scientific challenge in the discovery of this new phenomenon.

Flash-sintering is different from nominal field assisted sintering of ceramics. In field assisted sintering the rate of sintering is gradually enhanced as the applied field is increased, whereas in flash-sintering the event occurs precipitously. Nominal field

* Corresponding author.
E-mail addresses: marco.cologna@colorado.edu, marco_cologna@yahoo.it (M. Cologna).

0955-2219/$ – see front matter © 2011 Elsevier Ltd. All rights reserved.
doi:10.1016/j.jeurceramsoc.2011.07.004

assisted sintering in yttria doped zirconia has been successfully explained by the reduced rate of grain growth under the influence of an electrical field.[2,8]

The following possible mechanisms have been suggested for flash-sintering:

1. Local heating at grain boundaries: local resistance at particle–particle contacts can lead to higher local temperatures that enhances diffusion;[1]
2. Nucleation of Frenkel Pairs: nucleation of vacancy–interstitial pairs under the applied field. The applied field can strip the charge on the vacancy and the interstitial (an electron on one and a hole on the other), leaving them charge neutral relative to the lattice. The bias from the sintering pressure can then draw the vacancy preferentially into the grain boundaries and the interstitials into the pores, producing densification, while the electron–hole pair contributes to higher electrical conductivity.[9]
3. Interaction between external field and the space charge field: the field in the space charge layer adjacent to grain boundaries can have strength of 10–1000 V cm^{-1}. These values are comparable to the applied fields. The applied electric field may interact nonlinearly with the intrinsic fields, thereby changing the diffusion kinetics.[9]

In the present work we study the applicability of flash sintering to alumina, which, in contrast to the materials studied so far[1–6] is a poor electrical conductor. We show that fields higher than 500 V cm^{-1} trigger flash-sintering in MgO-doped alumina, while the same fields have little effect on the sintering of pure-alumina. As was the case in other ceramics,[1–6] the onset of flash-sintering in alumina is accompanied by a surge in the current. Therefore, phenomenologically speaking, MgO-doped alumina and yttria doped zirconia show the same "flash" effect even though one is essentially a stoichiometric compound while the other is highly non-stoichiometric.

2. Experimental

2.1. Flash-sintering

The setup for the flash-sintering experiments[1] is sketched in Fig. 1. This method is adapted from conventional sintering: the difference being that an electric field is applied by means of two platinum electrodes. The electrodes wires also serve the purpose of suspending the specimen into the hot-zone of the furnace. The change in the physical size of the sample is measured from pictures acquired with a CCD camera through an optical low pass filter and a silica window.[10] The shrinkage strain was calculated as the true strain, $\varepsilon = \ln(l/l_o)$, where ℓ is the time dependent gage-length and ℓ_o is the initial gage length.

In the present experiments a constant voltage was applied to the specimen, while the furnace temperature was increased at 10 °C min^{-1} up to 1400 °C, followed by an isothermal hold of 1 h. The current was limited at the power supply to 60 mA.

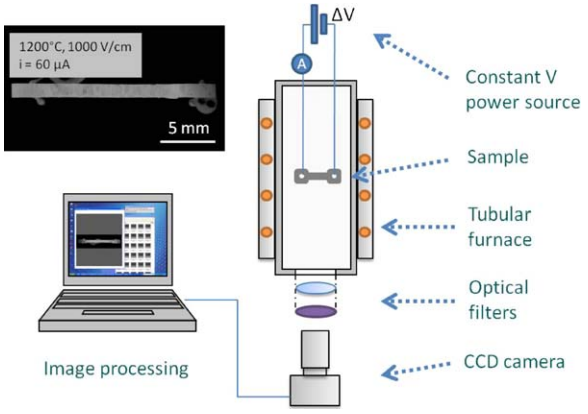

Fig. 1. Field-assisted sintering apparatus.

Often flash-sintering is seen during the ramp-up in the furnace temperature; the voltage supply was turned off just after this event.

2.2. Materials

The starting powder was AKP-50, High Purity Alumina from Sumitomo, specified to be >99.99% pure, and having a particle size of 100–300 nm. The powders were used either as-received, or doped with 0.25 wt% MgO. The doping was performed by adding the powder to a solution of magnesium nitrate and distilled deionized water.[11] The suspension was dried and ground in a mortar. The powder (doped or as received) was mixed with 5 wt% polyvinyl alcohol (mw 49,000, Fluka) in water. The slurry was dried at 90 °C in an oven and ground to a powder in mortar and pestle. The resulting powder was uniaxially pressed at 280 MPa in a dog bone shaped die, to a green density of 0.55 ± 0.01 of the theoretical density of α-Al_2O_3 (3.99 g cm^{-3}). The dimensions of the cold-pressed, green sample are given in Fig. 2.

For clarity, form here onwards the MgO-doped alumina is referred to as simply MgO–alumina. Experiments were also carried out with undoped, nominally pure-alumina. In these cases the material is simply called pure-alumina.

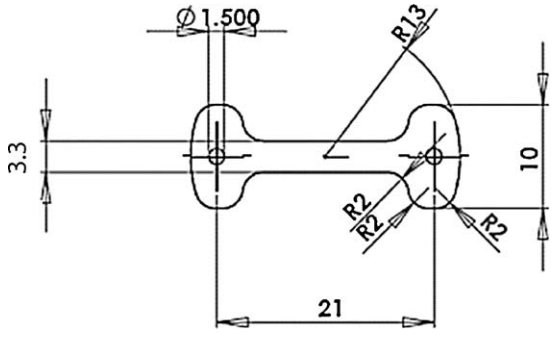

Fig. 2. Dimensions of the "green sample" in mm. The thickness of the samples was 1.8 mm.

2.3. DC electrical conductivity

The electrical current, or the dc electrical conductivity was measured in different types of experiments: (i) in the powder performs during the sintering process, (ii) in samples that had been sintered to full density by conventional sintering prior to the measurement of the conductivity, and (iii) by applying electrical fields of different amplitudes to samples prepared by conventional sintering, both as the applied fields were ramped up into the non-linear regime, and then lowered back down. The purpose of the last set of experiments was to determine if the non-linear increase in conductivity created defects that left a residual effect in the ceramic.

The temperature of the samples was raised (and then lowered) in steps of 50 °C between the range of 800 °C and 1400 °C, taking care that steady state current was achieved at each temperature before the measurement was taken, which usually occurred within 10 s. In some instances the field was applied for longer times, to study the current versus time profile. The specific conductivity is calculated according to the following relation:

$$\sigma = \frac{il}{Vwt} \quad (1)$$

where i is the measured current, V is the applied voltage, l the length, and w and t the width and the thickness of the gage section. The conductivity is calculated according to Eq. (1), by simplifying the geometry of the gage section to a constant cross section with initial dimensions of 3.3 mm × 1.8 mm × 20 mm.

The conductivity was measured in the two electrode configuration instead of the four point method, because it was difficult to apply four electrodes to a green sample undergoing sintering. The two electrodes test method is less accurate than the four point method because it includes the contact resistance. However, the two electrode method is likely to be valid provided the current reaches a steady state at constant field. Results reported later in the paper show that the steady state was reached in just a few seconds in the Ohmic regime. Also, the values of the conductivity we measure fall well within the nominal range reported in the literature.[12,13]

2.4. Microstructure

The grain size was measured from images taken with a JSM-7401F field emission SEM (JEOL). Specimens were prepared by thermal etching for 30 min at 1100 °C, followed by coating with a with a 2 nm layer of Au-Pd. The mean grain size was determined by the linear intercept method, with a correction factor of 1.56.

3. Measurements of strain and conductivity during the sintering process

3.1. Conventional sintering (without field)

The shrinkage strain versus temperature data for nominally pure and MgO–alumina without applied field (at 0 V) are given in Fig. 3. The temperature was ramped up to 1400 °C at a heating rate of 10 °C min^{-1} and then held at that temperature for 60 min. In both cases the final density is reached at a shrinkage strain of −0.18 which occurs at about mid-way during the holding period at 1400 °C. Both pure and MgO–alumina show similar sintering behavior. In the intermediate regime the doping has the effect of slightly delaying the sintering rate (upon reaching 1400 °C, the shrinkage of pure and MgO–Al_2O_3 are −0.135 and −0.115, respectively). However after 1 h isothermal hold, the sintering curves merge and the final shrinkage strains are nearly the same (−0.180 versus −0.178).

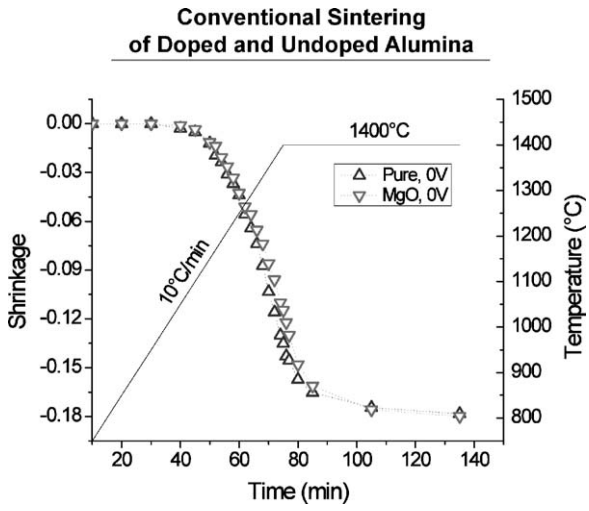

Fig. 3. Conventional sintering at a constant heating rate.

The use of MgO as a dopant is known to eliminate intragranular pores and refine the grain size, producing translucent alumina.[14] The effect of MgO on sintering rate is not new: in conventional sintering,[15] two steps sintering[16] and in spark plasma sintering,[17] MgO was observed to slightly retard densification in the intermediate stage of sintering, but to have a positive effect in the last stage of sintering. The segregation of MgO to grain boundaries is believed to retard the initial shrinkage,[15] and accelerate the final shrinkage[15] by preventing the breakaway of pores from the grain boundaries during grain growth.[18]

3.2. Field assisted sintering

The shrinkage curves for constant heating rate (10 °C min^{-1}) experiments are reported in Fig. 4. These experiments did not include an isothermal hold at 1400 °C. The data for pure-alumina is given on the left in figure (a), which are compared to the data for MgO–alumina on the right in (b). The data for 0 V (without field) is compared to the shrinkage behavior at field strengths of 250–1000 V cm^{-1}.

The data for pure-alumina in Fig. 4(a) shows that the sintering behavior with a field of 1000 V cm^{-1} is only very slightly higher than the sintering rate obtained in conventional sintering (without applied field). In either case full density is not reached at the end of the ramp up to 1400 °C (the microstructure confirms a porous structure). The shrinkage strains at the end of the experiments were −0.135 with the field, and 0.148 without the electrical field.

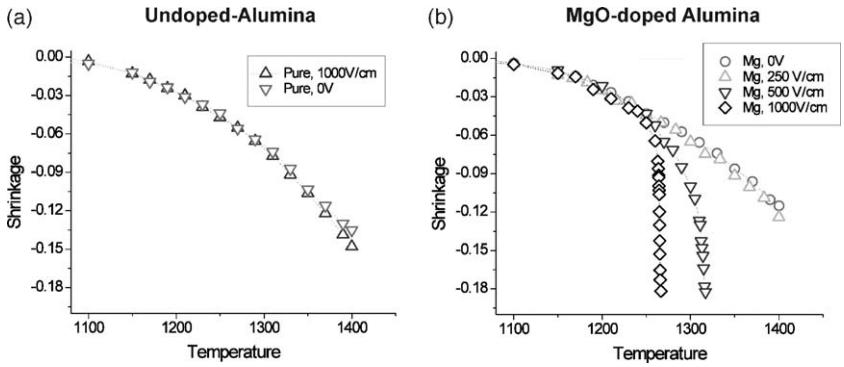

Fig. 4. Influence of applied electric field on the sintering behavior of pure-alumina (a), and doped alumina (b), in experiments carried out at a heating rate of 10 °C min^{-1}.

In contrast to pure-alumina, the dc field has a remarkable effect on the sintering of MgO–Al_2O_3. Three sets of data are given, at 250 V cm^{-1}, 500 V cm^{-1} and 1000 V cm^{-1}. The effect of the field is minor at 250 V cm^{-1}, with a strain of only −0.124 being achieved at 1400 °C. But at higher fields flash-sintering[1,3–7] is observed. At 500 V cm^{-1} full densification strain of −0.182 is obtained at 1320 °C, and at 1000 V cm^{-1} densification occurs at just 1260 °C. The shape of the sintering curves are noteworthy in that sintering follows the behavior seen in conventional sintering in Fig. 4(a), until the "flash event", when the sintering curves assume a nearly vertical posture, with full densification achieved within a few seconds. However, the curve for 500 V cm^{-1} suggests an incubation time for the onset of flash sintering, which is nearly absent, or very brief, at 1000 V cm^{-1}. It is possible that a slower rate of heating would shorten the incubation time. At 10 °C min^{-1} the lowest field for inducing flash sintering appears to be ∼500 V cm^{-1}, but it may be that lower heating rates can induce flash-sintering at lower fields.

3.3. Power dissipation

The power dissipation in the specimen is equal to the product of the applied voltage and the current flowing through the specimen. In earlier experiments with other oxides[1,3] we have found that the onset of flash-sintering is accompanied by a surge in power dissipation. The present experiments are consistent with this behavior. The data are plotted in Arrhenius form since the increase in (steady state) current with temperature is expected to be thermally activated, which, given a constant value for the activation energy, would appear as a straight line with a negative slope, since the experiments are carried out at a constant applied voltage. (This assumption is not strictly correct since the length and the cross-section of the specimen, as well as its porosity are changing as the sample sinters. However, the errors tend to cancel: for example while the gage length becomes shorter which would increase the specific conductivity, the cross section also shrinks which would decrease the conductivity. Although the cross-section decreases the conductivity at twice the rate as the length increases it – because the cross-sectional strain is twice the linear strain – this difference is further compensated by the reduction in porosity which would tend to increase the conductivity. These compensating effects justify the use of the initial dimensions of the specimen as an approximate estimate of the specific conductivity of the specimen while it sinters.)

We recall from Fig. 4 that a field of 1000 V cm^{-1} had little effect on the sintering behavior of pure-alumina, while it induced flash sintering at ∼1260 °C in MgO doped-alumina. This behavior is reflected in the Arrhenius plots of power-dissipation shown in Fig. 5b. While the pure-alumina follows an essentially Arrhenius behavior, the MgO–alumina exhibits a power surge that coincides with the onset of flash-sintering. The power dissipation curves for lower fields in MgO–alumina are given in Fig. 5b. A sharp increase in power-dissipation is seen at 500 V cm^{-1}, where flash-sintering is seen, but not at 250 V cm^{-1}, which did not appear to induce flash behavior. However, the slope of the curve at 250 V cm^{-1} deviates from linearity, unlike the data for the pure-alumina at 1000 V cm^{-1} given Fig. 5(a). This result suggests the onset of non-linear behavior to some degree at 250 V cm^{-1}, but not strong enough to precipitate flash-sintering which occurs when the field is increased to >500 V cm^{-1}. The hesitation in the power surge is evident even at 500 V cm^{-1}; it may reflect an incubation time for the onset of flash sintering seen in Fig. 4(b). In this respect that data appear to have a different exposition as compared to the earlier experiments with yttria doped zirconia where flash sintering occurred abruptly without an inkling of an incubation time.

Finally, it is to be noted that application of 1000 V cm^{-1} to the pure-alumina sample led to arcing and unstable conductivity when 1400 °C was reached. Perhaps the arcing would also have occurred in the MgO–alumina sample had it been ramped up to 1400 °C, but did not because sintering was completed at a lower temperature.

3.4. Microstructure

The microstructure of the specimens was examined in a scanning electron microscope. Specimens were prepared by thermal etching (30 min at 1100 °C) of the polished cross-section, followed by thin coating of Au-Pd. Two results (for MgO-doped alumina) are reported here. Both specimens had been sintered to full density, one in the conventional way, without an applied field at 1550 °C for 1 h, and the other flash-sintered at 1000 V cm^{-1} at 1260 °C. The micrograph from the flash-sintered specimen is

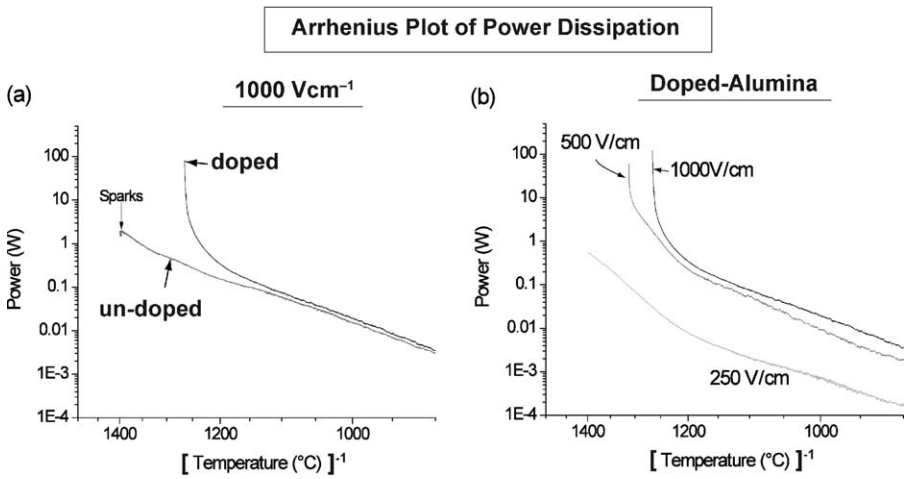

Fig. 5. Arrhenius plots for the power dissipation in the specimens in MgO and pure-alumina at the high field (a) and in MgO-alumina at different values of the applied field (b).

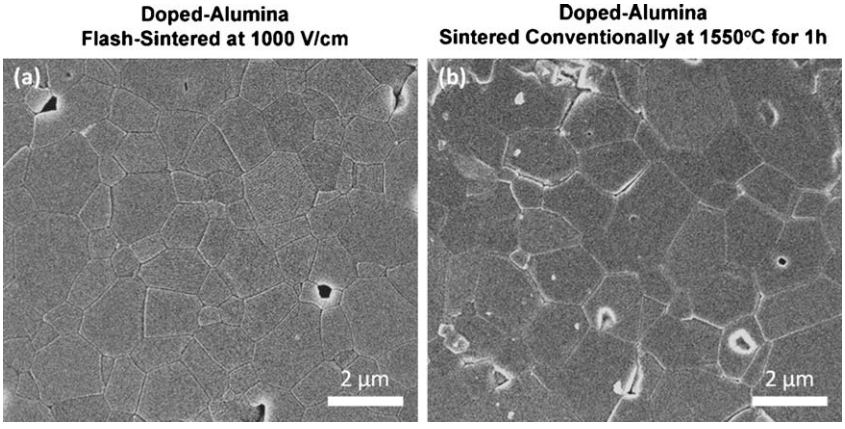

Fig. 6. Microstructures of flash-sintered and conventionally sintered MgO-doped alumina.

shown in Fig. 6(a), and from the conventionally sintered specimen in Fig. 6(b). The conventionally sintered specimen had an average grain size of 1.9 μm, while the flash-sintered specimen had a smaller grain size of 0.8 μm.

4. Conductivity of fully dense, conventionally sintered specimens

The measurements reported in this section were carried out on samples that had been sintered to full density, with and without MgO doping, at 1550 °C for 1 h, by conventional sintering. The green samples had the same shape as shown in Fig. 2, they were sintered without electric field in the same furnace configuration as in Fig. 1. The electrical conductivity was measured through the platinum wire electrodes attached to the specimen in the usual way.

The experiments were carried out by a stepwise increase in the temperature. At a given temperature the current was measured at different levels of the applied voltage. At each voltage the current was measured after it had reached a steady state, which usually happened in less than 25 s (but not in doped specimens at high fields, as explained later). In this way not only the effect of the temperature, but also non-linear (deviation from Ohmic) behavior, at higher fields, could be measured. Since the physical dimensions of the specimens were the same for all experiments, the measurement of the current and voltage are equivalent to the specific conductivity as prescribed by Eq. (1). The current at a given voltage was measured by holding the field constant for 25 s. The field was then removed for 5 s before stepping up (or down) to the measurement at the next voltage.

The most notable aspect of the results presented here is the non-linearity of the conductivity when they data are plotted with the expectation of Arrhenius behavior. Normally such a plot would exhibit linear behavior reflecting the following equation:

$$\sigma = Ae^{-\frac{Q}{RT}} \tag{2}$$

where σ is the conductivity, and Q is the activation energy for the conduction mechanism. Therefore, nominally, an Arrhenius plot of the conductivity yields a straight line with a slope that is a measure of the activation energy.

As reported below we see a stark difference between the Arrhenius plots for MgO-doped and pure-alumina. These plots are similar to the power-surges that were measured while the specimens were being sintered under an electrical field (Fig. 5).

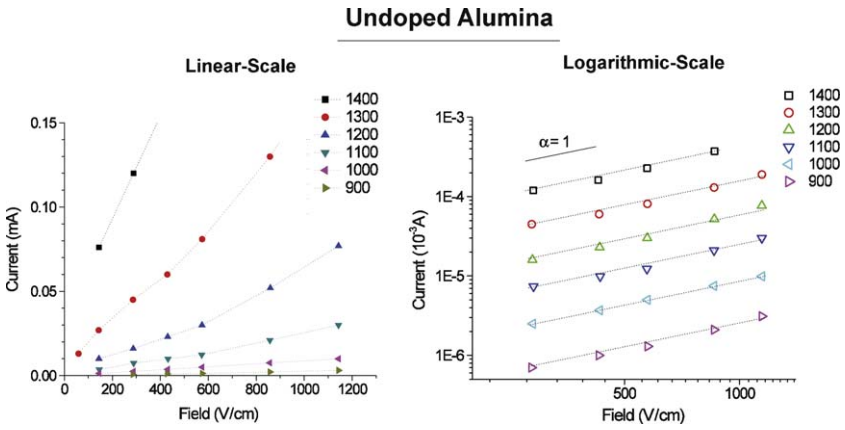

Fig. 7. Linear-scale and log-scale plots of the current versus the applied field for pure-alumina.

That this non-linearity is also seen in specimens that had been fully sintered in the conventional way proves that the non-linear power surge is not the cause of flash-sintering, but rather, it represents a phenomenon that shares the same mechanism as flash-sintering.

The non-linear behavior seen in the doped specimens (as described just above) was followed by measurements of the conductivity by first increasing and then decreasing the electrical field. The amplitude of the field was varied to assess the reversibility of the conductivity, especially when the amplitude was large enough to enter the non-linear regime. We see a remarkably high residual conductivity in specimens that had been subjected to high fields, suggesting that the non-linearity is accompanied by the nucleation of new charged defects, which survive when the current is measured again at lower applied fields.

The results below are reported in the following sequence: they start with the conductivity of pure-alumina, followed by the behavior of MgO–alumina, and finally results showing the residual conductivity in MgO–alumina which had been exposed to cyclic electrical fields are presented.

4.1. Conductivity of pure-alumina

The current–field (the *I–V*) plots for pure specimens at temperatures from 900 °C to 1400 °C, in steps of 100 °C, are given in Fig. 7. Plots using linear axes are shown on the left, and those with logarithmic axes on the right. The electric fields range up to 1000 V cm^{-1}, the same range that was used in the sintering experiments. At all temperatures, and for the full range of the electrical fields the plots are essentially linear. The non-linearity may be defined by the parameter α in the following equation:

$$i \propto E^{\alpha} \tag{3}$$

where $\alpha \approx 1$ implies linear behavior. The plots in Fig. 7(a) show small non-linearity at fields greater than 500 V cm^{-1}, which is likely from some Joule heating in the specimen. The log–log plots in Fig. 7(b), however, cannot distinguish the small non-linearity that is evident in (a).

The upward shift in the lines in the log-log plot as the temperature is increased reflects thermally activated conduction of charged defects. The Arrhenius plot of the conductivity at different temperatures is given in Fig. 8. All data fit into a reasonable straight line, whose slope yields and activation energy in the 150–207 kJ mol^{-1} range. Note this low value of the activation energy most likely precludes the possibility of ionic diffusion. In high likelihood, the conductivities being measured here are electronic conductivities. Since the metal electrodes do not block the transport of electrons across the metal-ceramic interface, we expect to reach the steady state current rather quickly, which was indeed the case (in less than a few seconds).

4.2. Conductivity of MgO-doped alumina in dense samples

The measurements of the conductivity in MgO–alumina was complicated by the non-linear behavior at fields greater than ~250 V cm^{-1}. In the non-linear regime a steady state value for the current could not be achieved within 25 s, indeed the current continued to increase with time. The field was increased in steps up to 750 V cm^{-1}. A dead period of 5 s was allowed between one field and the step up to the next field. At temperatures above 1200 °C and high fields, the current does not reach a steady state

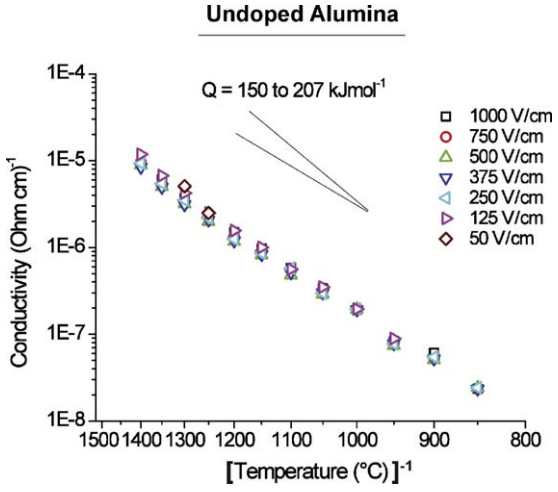

Fig. 8. Arrhenius plot of the conductivity of sintered pure Al_2O_3, measured under different dc fields.

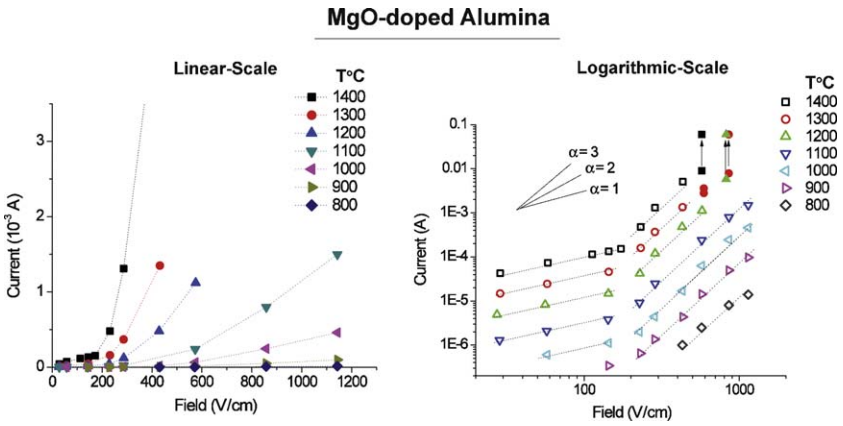

Fig. 9. Current as a function of the dc field in sintered MgO–Al_2O_3, at different temperatures.

but increased steadily to the maximum allowed by the power supply (60 mA).

The linear-scale and log–log plots for the current versus field are given in Fig. 9. They show that the behavior is essentially linear below ~200 V cm^{-1}, and non-linear above this field, regardless of the temperature.

Because of the wide spread in the values of the current, arising from the non-linear behavior, the log–log plots are more definitive in showing the transition to from linear to non-linear behavior. Note that the value for $\alpha \approx 1$ in the linear regime, but increases to $\alpha \geq 3$ in the non-linear regime. The slopes are temperature independent, and the transition between quasi-ohmic and non-ohmic behavior appears always at the same field intensity, regardless of the temperature. These results, for MgO–alumina, stand in contrast to the measurements for pure-alumina, that were reported in Fig. 8, where the behavior remained linear throughout the range of the applied field, at all temperatures.

The Arrhenius plot for the conductivity for MgO–alumina is shown in Fig. 10. It is to be contrasted to the data for pure-alumina that was presented in Fig. 8. The contrast is remarkable. Whereas, all the points, obtained at various levels of applied field, converge to a single line in pure-alumina, in the case of MgO–alumina the points spread out to different lines for different applied fields. However, the slopes for all the linear plots for MgO–alumina are the same as for pure-alumina, yielding similar activation energies. For MgO–alumina the activation energies lie in the range of 155–222 kJ mol^{-1}, while for pure-alumina they fall between 150–207 kJ mol^{-1}. There is a hint of two slopes at fields below 500V cm^{-1} – 155 kJ mol^{-1} below 1050 °C and 220 kJ mol^{-1} above 1050 °C – but the difference is not large enough to be definitive. At higher fields (above 500 V cm^{-1}) the data fit nicely to a single straight line throughout the temperature range with an activation energy of 210 kJ mol^{-1}.

The most significant distinction between the Arrhenius plots for pure and MgO–alumina is the dispersion in the lines for the data at different fields for MgO–alumina, but the coalescence of the data into a single line for the pure-alumina. In the doped case the lines move to higher values of the current as the field is increased. Despite the dispersion in the lines, the activation energies remain the same for all measurements. The results, therefore, show that the pre-exponential in Eq. (2) changes with the field in the MgO–alumina, but remains constant for pure-alumina. Since Q reflects the activation barrier for the mobility of the charged defects, while the pre-exponential is related to the concentration of the defects, we infer that the field has the effect of increasing the concentration of defects in MgO–alumina. This effect appears to be more pronounced above 500 V cm^{-1}, where there is a greater dispersion of the lines for the data in Fig. 10b, than below this field.

4.3. Residual conductivity after cycling MgO–alumina into the non-linear regime

We have hypothesized that the onset of non-linearity in conductivity arises from the increase in the defect concentration which enhances the pre-exponential in Eq. (2). If this is the case then it is also likely that some fraction of these defect concentrations survive when the applied field is traversed downwards. The results from these experiments are reported in this section. Indeed, they show considerable residual conductivity when the samples are cycled between increasing and decreasing applied

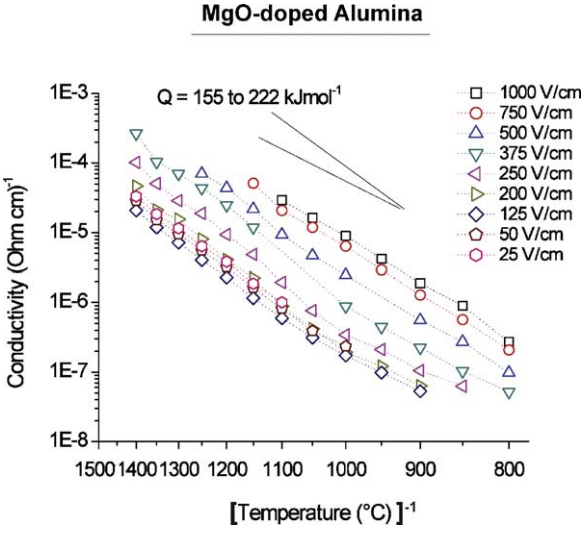

Fig. 10. Arrhenius plot of the conductivity of sintered MgO–Al_2O_3, measured under different dc fields.

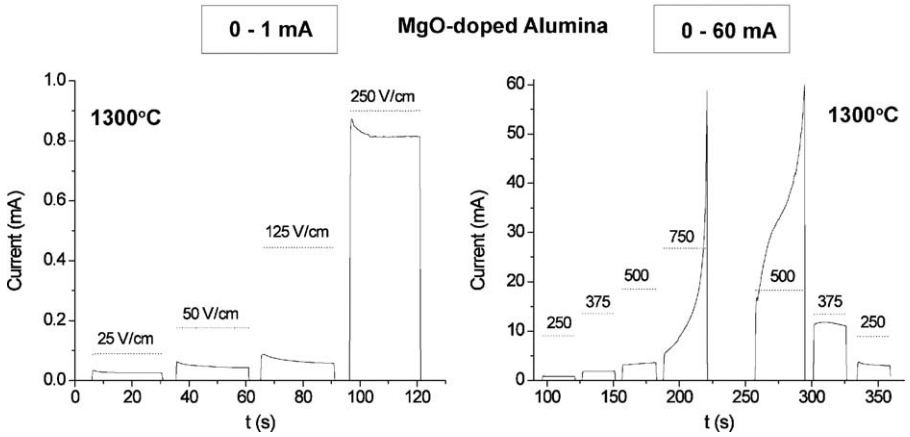

Fig. 11. Current as a function of the time in sintered MgO doped Al_2O_3, under a field of 25–250 V cm^{-1}, and 250–750 V cm^{-1}.

fields. This effect is seen only in the MgO–alumina; this is self-evident since pure-alumina did not exhibit non-linear increases in conductivity at high fields.

The time dependent change in the current, in a specimen held at 1300 °C, when the applied field is first increased in steps, up to 750 V cm^{-1}, and then stepped downwards, are given in Fig. 11. The field is held for 25 s at a given field, which is followed by a dead period of 5 s before the next step in the field is applied. The data are divided into two figures, the one on the left covers currents from 0–1 mA and the one on the right from 0–60 mA. The results for fields up to 250 V cm^{-1} are shown in the first figure and those for fields up to 750 V cm^{-1} in the second figure.

In the low field regime (up to 250 V^{-1}) the current usually decreases after the application of the field before settling down to a steady state. However, at fields ≥500 V cm^{-1}, the current continues to increase with time.

The data given on the right in Fig. 11, show the current-time profile when the applied field is stepped down from 750 V cm^{-1} to 500 V cm^{-1}, and then to 375 V cm^{-1}, and finally down to 250 V cm^{-1}. Note the much higher currents at these lower fields than were seen when the fields were being stepped upwards.

The hysteretic behavior described above is absent if the sample is not exposed to the non-linear regime. The results in Fig. 12 show the current–field behavior when the sample is cycled up and down in the applied field (here the applied voltage was changed continuously at a rate of 30 V s^{-1}). These experiments were carried out at 1300 °C, and a rest period of 30 s was allowed between the cycles. Three types of cycles were employed. In the first type the sample was raised to a field of 750 V cm^{-1}, in the second type of cycles the amplitude of the field was 600 V cm^{-1}, and in the third kind the maximum value of the field was limited to 300 V cm^{-1}. For the 750 V cm^{-1} case the current was cut-off at 60 mA (by the power supply) which is the reason for the "flat-top" for the value of the current. Note that the current is much higher during ramp-down than during the ramp-up part of the cycle. A similar behavior, though less severe, is seen when the field-amplitude was 600 V cm^{-1}. However, the behavior is linear and reversible when the amplitude was held at 300 V cm^{-1}. An expanded view of the data in the lower left corner of Fig. 12a is given on the right in Fig. 12b: it more clearly shows the linear and reversible behavior at low field-amplitude. The hysteretic behavior at the higher fields may not be attributed to Joule heating since the transition from reversible to hysteretic

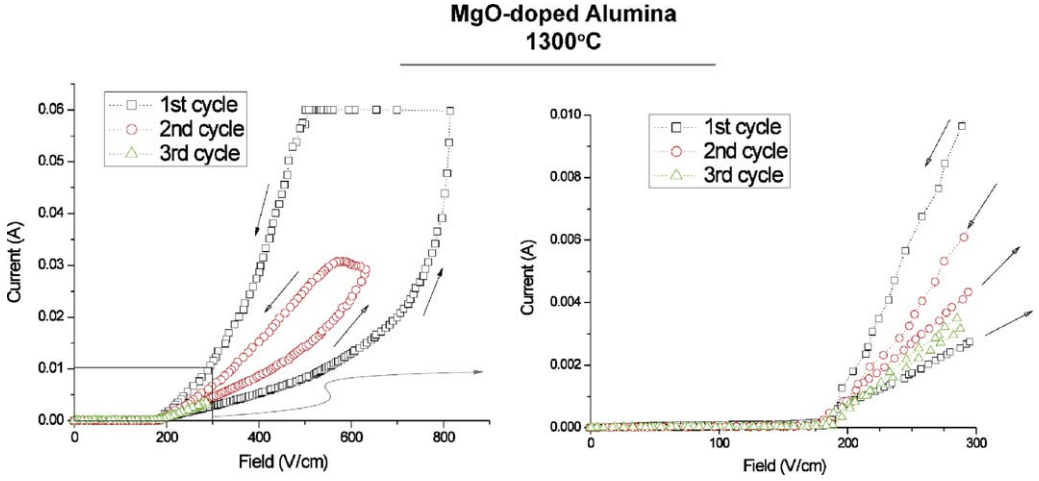

Fig. 12. Cyclic, current–field response upon the application of field controlled cycles of increasing amplitude.

shape of the cycles changes abruptly at a field of ~200 V cm^{-1}. The supposition is that defects introduced at the high fields lead to higher residual conductivity when the fields are brought back down.

5. Discussion of conductivity of alumina from the literature

The measurement of dc electrical conductivity of pure and MgO-doped alumina at high temperatures and high fields are unusual. They point towards electrons being the dominant transport species in both cases. A brief review of the reports from the literature are appropriate to give context to these measurements.

The values for dc conductivity of alumina reported in the literature vary over a wide range, and appear to depend greatly on purity and processing conditions.[13] Furthermore, the mechanism of conduction and the dominant charge carrier in Al_2O_3 have often been debated. In single crystal alumina it has been claimed to be predominantly electronic, ionic or mixed, and to depend on the temperature and oxygen partial pressure. For example, MgO doped Al_2O_3 single crystals have been reported to be electronic conductors at low temperatures and mixed ionic and electronic conductors at the higher temperatures and low p_{O2}.[19] At high temperatures the ionic conduction is explained by Al interstitials[20] or oxygen vacancies at low p_{O2}, while the electronic conduction is dominated by holes.[21] More recent results attribute only 0.3% of the conductivity in pure single crystals at 1200 °C to arise from ionic diffusion.[22] The measurement of the activation energy in the present experiments suggest electronic conductivity in both doped and pure-alumina at fields up to 200 V cm^{-1} in the temperature range of 800–1400 °C.

The non-linear conductivity of MgO-doped alumina seen at fields 250–1000 V cm^{-1} at temperatures up to 1400 °C, as measured in the present experiments, has not (to our knowledge) been reported in the literature, although a non-linear *I–V* behavior has been seen in thin films of alumina at low temperatures. In a recent paper Talibi[23] shows a transition from Ohmic to "super-Ohmic" behavior in 0.65 nm thick 96% pure Al_2O_3 film at low temperatures, but at fields much higher than those employed in the current experiments. The non-linearity was explained by space charge limited conduction. In a different study on 490 nm thick films of porous alumina the transition from quasi-Ohmic to superOhmic behavior was observed at 204 kV cm^{-1} at room temperature.[24] The conduction mechanism was attributed to electron-hopping at low fields, and space charge limited conduction in the high field regime.

The conductivity in alumina is also known to increase in the presence of ionizing radiation.[25,26] The radiation induced conductivity (RIC), or radiation induced degradation (RID), increased dramatically at fields above a threshold of 500 V cm^{-1}.[26] This result was explained by an increase in the stable F-center production rate by means of either an increase in the primary vacancy-interstitial production rate or a decrease in the recombination rate.[26] This non-linear effect of the fields on conductivity at fields similar to those in the current experiments is to be noted, as is the equivalence between the nature of radiation damage and the nucleation of Frenkel pairs that is postulated to explain flash-sintering.

An interesting effect of a dc field on the conductivity of MgO has been well documented.[27–29] A field of 1000 V cm^{-1} was applied for ~100 h at 1200 °C. The conductivity of MgO remained constant at first, but then started to increase eventually by three orders of magnitude leading to Joule heating and electrical breakdown. This incubation time for the increase in conductivity was explained by the piling up of cation impurities and lattice defects in the vicinity of dislocations and small angle grain boundaries. Perhaps a similar aggregation of defects along the grain boundaries in Al_2O_3 could have been responsible for the results reported from the current experiments.

6. Summary

Pure-alumina, of nominal purity does not show field–assisted sintering under the conditions where MgO-doped alumina does. The transition from a gradual enhancement in sintering rate to flash-sintering seen in yttria-stabilized zirconia, with increasing field, is not observed in MgO-alumina. In alumina the effect of field on the sintering rate is unremarkable below a threshold field. This threshold field is ~500 V cm^{-1}. Flash sintering is recorded at and above this threshold field.

The onset of flash-sintering is accompanied with a non-linear increase in the conductivity of the specimen. This power surge was also seen in yttria-stabilized zirconia. However, an incubation time for this onset is present in MgO-alumina which was not observed in yttria-stabilized zirconia.

The conductivity of the alumina samples was measured in conventionally sintered, fully dense samples of the non-linear increase in conductivity with applied field that was seen during flash-sintering was also present in these dense samples. The effect of doping was similarly reflected in these measurements: the pure samples, which did not exhibit field assisted sintering also did not show non-linear behavior in conductivity.

The conductivity data for the pure samples remained Ohmic and well behaved over the full range of fields and temperatures in the present study. All data conformed to approximately a single valued activation energy, which was in the range of 170–225 kJ mol^{-1}. These activation energies are far too low for ionic diffusion. The inference is that the conductivity in the present experiments was dominated by electrons and holes. The easy and quick attainment of steady state current upon application of the electric field via platinum electrodes is also consistent with the non-blocking nature of these electrodes for electronic conduction.

The conductivity of the MgO-doped samples could be separated into two regimes: below ~200 V cm^{-1} the behavior remained linear. However, at higher field the currents increased in a highly non-linear fashion. Furthermore, when the field was cycled up and down, the current during the downward portion of the cycle was greater than when the field was being increased. This hysteretic behavior became increasingly pronounced as the amplitude of the applied field was increased. The cyclic behavior was fully reversible and linear when the amplitude was kept less than 200 V cm^{-1}.

The activation energy plots for conductivity in the MgO-doped samples bore similarity with, but also differed from those for the pure samples. In pure-alumina the data for all fields and temperature conformed to a single line on an Arrhenius plot. In the MgO-alumina, the data for a single value of the applied field did fit an approximate straight line, but these lines shifted parallel to one another, and upwards to higher conductivities as the field was increased. Interestingly the slope of these lines, that is the activation energy, matched the value measured for the pure samples. It is inferred that activation energy for the diffusion of conducting species was left unchanged by the applied field, but the pre-exponential which is proportional to the concentration of the charge defects increased with the applied field in the doped samples.

The confluence of the onset of non-linear conductivity (in fully dense samples) and the onset of flash-sintering in field assisted sintering experiments is noteworthy. Normally, the conductivity and sintering of ceramics is controlled by different diffusion transport mechanisms. The conductivity is determined by the fastest moving charge species, while sintering is controlled by the transport of charge neutral molecules whose overall diffusivity is controlled by the slowest moving charged species in the molecule. It follows, that the mechanism that is proposed for the flash-sintering phenomenon must explain this dichotomy between transport kinetics for charge conduction and sintering.

The nucleation of Frenkel pairs under the applied field is proposed as a possible mechanism to explain the above dichotomy. In this mechanism a vacancy and an interstitial are created simultaneously for both the cations and the anions. The Frenkel pairs carry opposite charge relative to the lattice, one carrying an electron and the other a hole. It is proposed that the electrons and the holes are separated from these defects under the applied field which renders the vacancies and the interstitials to become charge neutral relative to the lattice thereby enhancing their mobility. The bias from the sintering pressure then pulls the interstitials preferentially into the pores and the vacancies into the grain boundaries leading to densification. In this way the electronic conductivity becomes coupled to the sintering kinetics.

The difference in the conductivity and sintering behavior of MgO-doped alumina and alumina of nominal purity is highly remarkable, and difficult to explain at this point. It is known that MgO has limited solubility in alumina, and that it segregates to the grain boundaries at relatively low overall concentrations. At low applied fields the pure and MgO-alumina have very similar conductivities, and exhibit similar sintering kinetics. But at high fields the properties diverge with the MgO-alumina exhibiting flash-sintering as well as non-linear conductivity, while the pure-alumina remains well behaved. The similar conductivity of the two aluminas at low field makes it unlikely that MgO is influencing the electronic conductivity of alumina—its effect appears to be on the non-linear behavior. If the Frenkel defect nucleation mechanism were to hold, then its effect must be related to this nucleation mechanism. One possibility is that the dopant creates local amplifications in the electrical fields which enhance the probability for the nucleation of Frenkel pairs.

Acknowledgements

This work was financially supported by theBasic Energy Sciences Division of the Department of Energy under Grant no.: DE-FG02-07ER46403.

References

1. Cologna M, Rashkova B, Raj R. Flash sintering of nanograin zirconia in <5 s at 850 °C. *J Am Ceram Soc* 2010;**93**(11):3556–9.
2. Yang D, Raj R, Conrad H. Enhanced sintering rate of zirconia (3Y-TZP) through the effect of a weak dc electric field on grain growth. *J Am Ceram Soc* 2010;**93**:2935–7.
3. Cologna M, Prette ALG, Raj R. Flash-sintering of cubic yttria-stabilized zirconia at 750 °C for possible use in SOFC manufacturing. *J Am Ceram Soc* 2011;**94**(2):316–9.
4. Prette ALG, Cologna M, Sglavo VM, Raj R. Flash-sintering of Co_2MnO_4 spinel for solid oxide fuel cell applications. *J Power Sources* 2011;**196**:2061–5.
5. Raj R. *Investigating the influence of electrical fields on sintering and related phenomena in ceramics using the sinter-forging method*. 2010.
6. Karakuscu A, Cologna A, Blas U, Raj R. unpublished work.
7. Francis J, Raj R. Flash-sinterforging of nanograin zirconia: field assisted sintering and superplasticity. J Am Ceram Soc (in press).
8. Ghosh S, Chokshi AH, Lee P, Raj R. A huge effect of weak dc electrical fields on grain growth in zirconia. *J Am Ceram Soc* 2009;**92**: 1856–9.
9. Raj R, Cologna M, Francis JSC. Influence of externally imposed and internally generated electrical fields on grain growth, diffusional creep, sintering and related phenomena in ceramics. *J Am Ceram Soc* 2011;**94**(7): 1941–65.
10. Cologna M, Bertoldi M, Sglavo VM. Curvature upon co-sintering of anode supported solid oxide fuel cells. *Int J Appl Ceram Technol* 2010;**7**(6):803–13.
11. Venkatachari KR, Raj R. Shear deformation and densification of powder compacts. *J Am Ceram Soc* 1986;**69**:499–506.
12. Bauer AA, Bates JL. *Battelle Mem Inst Rept* 1930 (July 31, 1974).
13. Kingery WD, Bowen HK, Uhlmann DR. *Introduction to ceramics*. New York: Wiley; 1976, 903 p.
14. Coble RL. U.S. patent no. 3,026,210 (1962).
15. Jorgensen PJ. Modification of sintering kinetics by solute segregation in Al_2O_3. *J Am Ceram Soc* 1965;**48**:207–10.
16. Lin FJT, De Jonghe LC, Rahaman MN. Initial coarsening and microstructural evolution of fast-fired and MgO-doped Al_2O_3. *J Am Ceram Soc* 1997;**80**(11):2891–6.
17. Shen Z, Johnsson M, Zhao Z, Nygren M. Spark plasma sintering of alumina. *J Am Ceram Soc* 2002;**85**(8):1921–7.
18. Berry KA, Harmer MP. Effect of MgO solute on microstructure development in Al_2O_3. *J Am Ceram Soc* 1986;**69**(2):143–9.
19. Wang HA, Lee CH, Kröger FA, Cox RT. Point defects in α-Al_2O_3: Mg studied by electrical conductivity, optical absorption, and ESR. *Phys Rev B* 1983;**27**:3821–41.
20. Brook RJ, Yee J, Kröger FA. Electrochemical cells and electrical conduction of pure and doped Al_2O_3. *J Am Ceram Soc* 1971;**54**(9): 444–51.
21. Mohapatra SK, Kröger FA. Defect structure of α-Al_2O_3 doped with magnesium. *J Am Ceram Soc* 1977;**60**(3–4):141–8.
22. Will FG, deLorenzi HG, Janora KH. Conduction mechanism of single-crystal alumina. *J Am Ceram Soc* 1992;**75**(121):295–304.
23. Talbi F, Lalam F, Malec D. DC conduction of Al_2O_3 under high electric field. *J Phys D: Appl Phys* 2007;**40**:3803–6.
24. Karahaliou PK, Theodoropoulou M, Krontiras CA, Xanthopoulos N, Georga SN, Pisanias MN. Transient and alternating current conductivity of nanocrystalline porous alumina thin films on silicon with embedded silicon nanocrystals. *J Appl Phys* 2004;**95**(5):2776–80.

25. Pells GP. Radiation-induced degradation of the intrinsic electrical conductivity of $MgAl_2O_4$ and Al_2O_3. *J Nucl Mater* 1991;**184**:177–82.
26. Hodgson ER. Radiation enhanced electrical breakdown in $A1_2O_3$: field effect. *Nucl Instrum Methods Phys Res* 1992;**B65**:298–300.
27. Narayan J, Weeks RA, Sonder E. Aggregation of defects and thermal-electric breakdown in MgO. *J Appl Phys* 1978;**49**(12):5977–81.
28. Sonder E, Kelton KF, Pigg JC, Weeks RA. The effect of electric current on the conductivity of MgO single crystals at temperatures above 1300 K. *J Appl Phys* 1978;**49**(12):5971–6.
29. Evans BD. A review of the optical properties of anion lattice vacancies and electrical conduction in $-A1_2O_3$: their relation to radiation-induced electrical degradation. *J Nucl Mater* 1995;**219**:202–23.